A Conformational Study by ^1H NMR of a Cyclic Pentapeptide Antagonist of Endothelin

Murray Coles, Victoria Sowemimo, Denis Scanlon,† Sharon L. A. Munro, and David J. Craik*

School of Pharmaceutical Chemistry, Victorian College of Pharmacy, 381 Royal Parade, Parkville, Victoria, Australia 3052, and CSIRO Animal Health Laboratory, Geelong, Victoria, Australia 3220

Received January 22, 1993

The selective endothelin antagonist cyclo(D-Glu-L-Ala-D-allo-Ile-L-Leu-D-Trp, BE18257B) has been synthesized via solid-phase methods and its solution conformation determined by NMR spectroscopy and simulated annealing calculations based on NOE constraints. Additional information used in the structure determination included coupling constants and chemical-shift measurements as a function of temperature. The chemical shifts of two of the NH protons (D-Glu and D-Ile) exhibit low sensitivity to changes in temperature, indicating their involvement in hydrogen-bonded interactions. The main features of interest in the solution conformation include the presence of both a type-II β-turn and an inverse γ-turn, with central hydrogen bonds between H_N of D-Glu_1 and the C=O of D-allo-Ile_3 and between H_N of D-allo-Ile_3 and the C=O of D-Glu_1. The correlation of this solution conformation to the peptide's biological activity is discussed. The data are also compared with recently derived structures for BQ123, cyclo(D-Asp-L-Pro-D-Val-L-Leu-D-Trp), another highly potent endothelin antagonist. The backbone conformations of the two cyclic peptides are found to be similar. Comparisons with literature structure–activity data suggest that these peptides may mimic structural features of the C-terminal tail of the endothelins.

I. Introduction

Endothelin is a recently discovered vasoactive peptide which has attracted considerable interest from the pharmaceutical industry because of the possibility of designing antagonists which may be useful in a number of illnesses, including cardiovascular disease, renal disease, and asthma.[1] As a result of the importance of this peptide, there have been a number of studies of the solution structure of endothelin. On the one hand, elements of secondary structure have been detected in various studies,[2-6] but on the other, the notion that the peptide is conformationally flexible in some regions has also been proposed.[1-6] In the design of antagonists it has therefore been of interest to consider constrained molecules, and to this end a number of cyclic peptides have been identified which have significant antagonist activity.[7]

The cyclic pentapeptide cyclo(D-Glu-L-Ala-D-allo-Ile-L-Leu-D-Trp; BE18257B, see Figure 1) was recently isolated independently by Nakajima et al.[7] and Miyata et al.[8] from cultured broths of streptomyces species bacteria and has subsequently been shown to be a highly selective antagonist at the ET_A receptor.[9] Structure–activity studies utilizing this peptide as a lead compound have begun appearing in the literature.[10] Studies of the three-dimensional conformation of this peptide should assist in a better understanding of the structural requirements at the ET_A receptor and, hence, in the development of both nonpeptidic and peptidic antagonists. Potent ET_A antagonists have the potential to play multiple therapeutic roles as well as to be useful research aids to assess the physiological and pharmacological roles of the endothelin peptide family.

The current study was designed to synthesize BE182578 and examine its conformation in solution. The aim of the work was to generate structural information that would be useful in defining the relationship between structure, conformation, and activity. The study was carried out using a combination of 2D NMR methods at 300, 500, and 600 MHz. Data collected included studies of the temperature dependence of the NH chemical shifts, NOE experiments and coupling constant measurements. From this information, a proposed solution structure of this novel antagonist has been derived using molecular dynamics calculations.

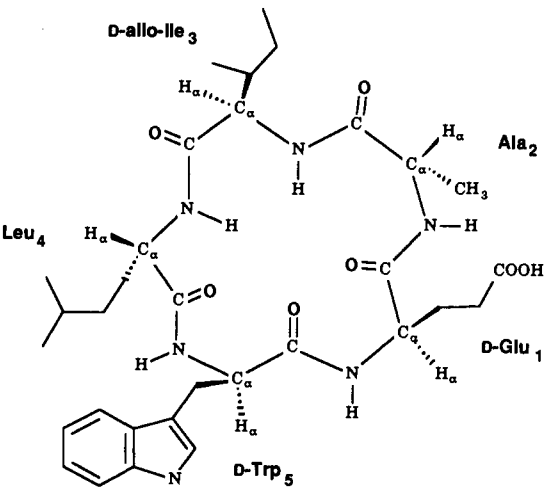

Figure 1. Molecular structure of cyclo(D-Glu-L-Ala-D-allo-Ile-L-Leu-D-Trp), BE18257B, indicating residue labeling.

II. Experimental Section

Materials. The linear peptide was synthesized by Fmoc solid-phase peptide synthesis methodology[11] on Fmoc-L-Ala-Wang resin,[12] cleaved with TFA/phenol (95:5), and cyclized in solution. The cyclic peptide was purified by reversed-phase HPLC and characterized by PITC amino acid analysis and FAB mass spectrometry (MH^+ 613). Details of the synthetic protocol will be published elsewhere.

NMR Methods. Samples for NMR spectroscopy were prepared by dissolving approximately 1.8 mg in 0.5 mL of DMSO-d_6, i.e., approximately 6 mM in a 5-mm external diameter sample tube (Wilmad Glass Company, 535-PP grade). ^1H NMR spectra were acquired at 300, 500, and 600 MHz on Bruker AMX 300, AMX 500, and AMX 600 spectrometers, respectively. 300-MHz

* Author to whom correspondence should be addressed.
† CSIRO Animal Health Laboratory.

0022-2623/93/1836-2658$04.00/0 © 1993 American Chemical Society

spectra (DQF-COSY[13], 300 ms NOESY[14] and 120 ms TOCSY[15]) were recorded at 318 K with a spectral width of 4505 Hz. 500-MHz spectra (80 ms TOCSY and 300 ms NOESY) were recorded at 295 K with a spectral width of 6205 Hz. A 300-ms NOESY spectrum was also acquired at 293 K at 600 MHz with a spectral width of 6098 Hz. The TPPI method of acquisition was used in all cases. The signal due to residual H_2O was suppressed by continuous low-power irradiation of the carrier frequency during a 2.5–3-s relaxation delay and during the NOESY mixing time. Data matrices typically consisted of 2048 complex points in F_2 (4096 for DQF-COSY) for each of 300-512 F_1 increments, the data being zero-filled to a 2048 × 2048 complex matrix before transformation. The apodization functions used in processing were an 80° or 90° shifted sine-bell squared for NOESY spectra and similar functions shifted by, typically, 60° or 70° for TOCSY and DQF-COSY spectra. 2D spectra were processed using the FELIX program[16] on a Silicon Graphics IRIS 4D/30 workstation.

Simulated Annealing. The data derived from the NMR spectra were analyzed via *in vacuo* molecular dynamics simulations using XPLOR 3.0[17] on a Silicon Graphics IRIS 4D/30 workstation. Due to the nature of the small, cyclic peptide system, some modifications to the standard XPLOR simulated annealing protocol were necessary. In particular, the possibility of deviations from planarity of peptide bonds[18] and the existence of backbone ϕ and ψ torsion-angle combinations from high-energy regions of the Ramachandran map necessitated some minor modifications of the XPLOR force field parameters. The standard force field parameter set used for simulated annealing calculations (PARALLHDG.PRO) contains inflated force constants designed to maintain covalent geometry during high-temperature stages of the simulation.[17] For example, the force constant maintaining peptide bond planarity, which was set to 8.2 kcal/mol/rad in the original CHARMM force field supplied with XPLOR 3.0, had been increased to 500 kcal/mol/rad. Under these conditions, the calculation of structures with nonplanar peptide bonds is unlikely. After some experimentation, a value of 50 kcal/mol/rad for this force constant was found to be adequate to prevent the conversion of *trans* to *cis* peptide bonds during the simulated annealing while allowing access to conformations where peptide bond planarity deviated by ±10°.

In a final refinement stage, the preliminary structures calculated using the modified parameter set were relaxed under the influence of the more complete PARAMALLH3X.PRO parameter set,[17] where the force constant on peptide bond rotation was set to 8.2 kcal/mol/rad (the experimental barrier). In order to allow access to conformations associated with high-energy regions of the Ramachandran map, 1–4 nonbonded interactions were calculated explicitly, i.e., force constants on dihedrals around rotatable bonds were set to 0, and 1–4 interactions were included in all the above calculations by setting NBXMOD = 3.

The considerations above were utilized in structure determination using a slightly modified version of the standard XPLOR protocol.[17] Starting structures were generated by subjecting a structure created by randomizing atom coordinates to a combination of dynamics and energy minimization. This procedure yielded a "template" with essentially random torsion angles but with correct covalent geometry and low nonbonded energy. The simulated annealing protocol consisted of five stages, as follows:

Stage 1. Fifty cycles of minimization under constraints with the force-field terms relating to covalent geometry modified as described above. Parameters determining the modeling of nonbonded interactions were set such that electrostatic terms are neglected (repel = 1) and atoms are able to pass through one another (vdw = 0.002). The force constant on the NOE constraints was lowered by setting the asymptote of the soft-square potential function to 0.1.

Stage 2. Six ps of dynamics at 600 K under the same nonbonded conditions as above, but with angle and improper terms modified by a factor of 0.4 and 0.1, respectively.

Stage 3. A further 3 ps of dynamics with the asymptote of the NOE term increased to 1 and weights on covalent geometry terms returned to their full values. During the first three stages, the cyclic structure was opened by replacement of the Ala_2 to Ile_3 peptide bond with a pseudo-NOE constraint to allow wider sampling of conformational space. This peptide bond was reformed at the end of this stage.

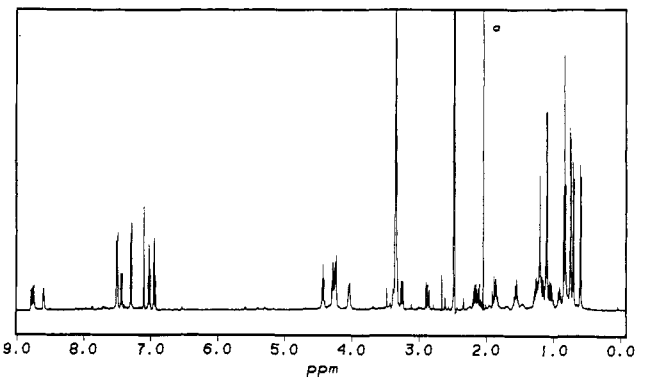

Figure 2. 600-MHz one-dimensional ^1H NMR spectrum of BE18257B in DMSO. The sharp peak at approximately 2.1 ppm, marked a, is due to residual acetonitrile in the peptide sample.

Table I. ^1H NMR Chemical Shifts (ppm) of BE18257B in DMSO[a,b]

residue	NH	Hα	Hβ	others
D-Glu_1	7.49	4.26	1.86	γ 2.11
L-Ala_2	8.65	4.44	1.13	
D-allo-Ile_3	7.44	4.29	1.57	γ 1.30, 1.09, γ_2 0.81, δ 0.89
L-Leu_4	8.53	4.07	1.21	γ 1.00, δ 0.77, 0.67
D-Trp_5	8.69	4.30	β^2 2.92, β^3 3.27	2H 7.12, 4H 7.54, 5H 6.99, 6H 7.07, 7H 7.31

[a] Chemical shifts are referenced to TMS at 0.0 ppm. [b] Spectrum was recorded at 293 K and 500 MHz.

Stage 4. The system was cooled to 100 K via 3 ps of dynamics during which the nonbonded parameters were increased linearly from repel = 0.9–0.75 and vdw = 0.003–4.0.

Stage 5. Two hundred cycles of energy minimization using the Powell algorithm.

The procedure of opening and closing the cyclic structure was carried out to avoid any bias in the range of backbone torsion angles sampled during the equilibration dynamics.[19] Structures produced by the above protocol were refined by reapplication of stage 4 over 10 ps using both a higher initial temperature (2000 K) and the square potential well for NOE constraints. Finally, the structures were relaxed via 1200 steps of minimization using the modified PARMALLH3X.PRO force field described above. Twenty structures were generated for each of two starting structures to give a final set of 40 structures. The two sets were used to avoid any possible bias the starting structure may have had on the calculations. No significant difference in either total energy or violation of NOE constraints was observed for the two sets.

III. Results

NMR Spectroscopy. Figure 2 shows the 1D spectrum of BE18257B in DMSO at 293 K. The spectrum is generally well dispersed, except for overlap of two of the five α-protons. Two-dimensional methods were used to make definitive assignments for the various protons; this was completed using a combination of DQF-COSY, TOCSY, and NOESY experiments.[20] The assignments are summarized in Table I.

Distance constraints for BE18257B were derived from NOESY spectra. It is common for molecules of this size to give little or no observable NOESY cross-peak intensity, as their correlation times are close to the extreme narrowing limit. In order to use NOESY spectra to estimate interproton distances in BE18257B, it was necessary to establish temperature and magnetic field conditions which gave the maximum observable NOESY cross-peak intensity. This procedure was preferred to the alternative of running ROESY spectra because of potential complications in the derivation of distance constraints from ROESY

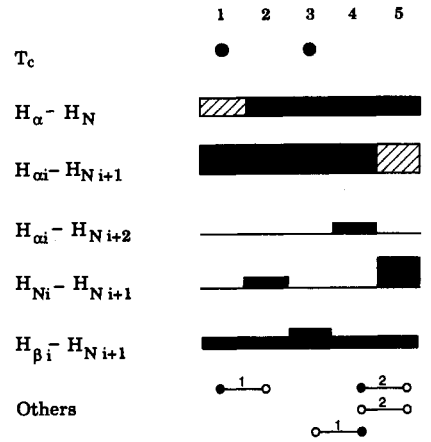

Figure 3. Summary of the observed NOE connectivities. The observed NOE's are classified into three levels quantified by the height of the bars. Hatched bars indicate where quantitation of intensities was not possible due to spectral overlap. T_c (temperature coefficients) are marked for those residues where the $T_c < -2$ ppm/1000 °C. Inter-residue NOE's observed are also marked. Filled and open circles represent connectivities between backbone and side chain protons, respectively. The number of occurrences of each type is given above the bar.

Table II. $^3J_{HN\text{-}\alpha}$ Coupling Constants Observed for BE18257B in DMSO[a]

amino acid	obsd $^3J_{HN\text{-}\alpha}$ (Hz)	θ[b] calcd[d]	θ[b] constraint[e]	ϕ[c]
D-Glu$_1$	7.6	-147, 147	150	90
L-Ala$_2$	7.8	-149, 149	-150	-90
D-allo-Ile$_3$	9.5	-170, 170	170	130
L-Leu$_4$	6.3	-136, 136, -20, 20	-135	-75
D-Trp$_5$	8.3	-153, 153	155	95

[a] Coupling constants were measured from a 1D spectrum recorded at 293 K and 600 MHz. [b] θ: HN-N-C_α-H_α. [c] C-N-C_α-C, resulting from constraint on θ. [d] Calculated from the Karplus relationship. [e] The value to which the torsion angle was constrained (±30°) during the molecular dynamics calculations.

data.[21] Temperature and magnetic field conditions for test NOESY spectra were chosen in an effort to achieve correlation times significantly different to the extreme narrowing limit. A correlation time faster than this limit was obtained by increasing temperature at low field (300 MHz, 318 K), resulting in observable cross-peaks opposite in phase to the diagonal. However, the maximal intensity was observed in a NOESY spectrum acquired at the highest available field and at the lowest practical temperature (600 MHz, 293 K), where the correlation time was increased beyond the extreme narrowing limit. In this case, cross-peaks had the same phase as the diagonal. This was the spectrum used to derive distance constraints.

A summary of the observed NOE connectivities is shown in Figure 3. The upper limits of interproton distances were estimated as 2.6, 3.2, 4.0, and 5.0 Å on the basis of intensities for strong, medium, weak, and very weak NOESY cross-peaks, respectively, with appropriate allowance for pseudoatoms where necessary. This analysis resulted in 45 conformationally dependent distances which were used as upper constraints in molecular dynamics simulations.

Coupling constants were also measured to provide information about torsion angles within the structure. $^3J_{NH\alpha}$ coupling constants are recorded in Table II. The magnitudes of these coupling constants fall in the range 6.3–9.5 Hz and would normally therefore be considered to represent averages over several conformations. In the current case this is unlikely, as the peptide is cyclic and hence these couplings represent a defined conformation or, at worst, an average over a range of similar conformations. Analysis of the couplings using the Karplus equation adapted for peptides[20] yielded a series of torsion angles, shown in Table II. Because of the sinusoidal nature of the Karplus equation there are two solutions for a given coupling, but because of the cyclic nature of this system, only one of these is physically reasonable for any particular case. The torsion angles listed in Table II were used as constraints in the simulated annealing calculations. These constraints were applied with a tolerance of ±30° and a force constant of 1 kcal/mol/rad^2. Consideration of $^3J_{\alpha\beta}$ coupling constants and NOESY cross-peak intensities allowed the stereospecific assignment of the prochiral β-methylene resonances[22] of Trp$_5$ (as shown in Table I) and subsequent analysis of the relative populations of the three staggered conformations around Trp$_5$ χ_1. The observed coupling for these protons is Hβ^2 ($^3J_{\alpha\beta}$ = 2.7 Hz) and Hβ^3 ($^3J_{\alpha\beta}$ = 11.9 Hz) which, in principle, represents average values over the three staggered rotamers. Analysis of the relative populations of these rotamers was done by comparison of the observed values with the ideal values for the pure rotamer values J_{gauche} = 2.6 Hz and J_{trans} = 13.6 Hz.[23] This analysis indicates that the rotamer corresponding to $\chi_1 = 180°$ is effectively unpopulated and that the population of the remaining two rotamers is, within experimental error, more than 80% for $\chi_1 = +60°$ and less than 20% for $\chi_1 = -60°$. This information was not used in constraining the simulated annealing calculations but was subsequently found to be in agreement with the calculated structures.

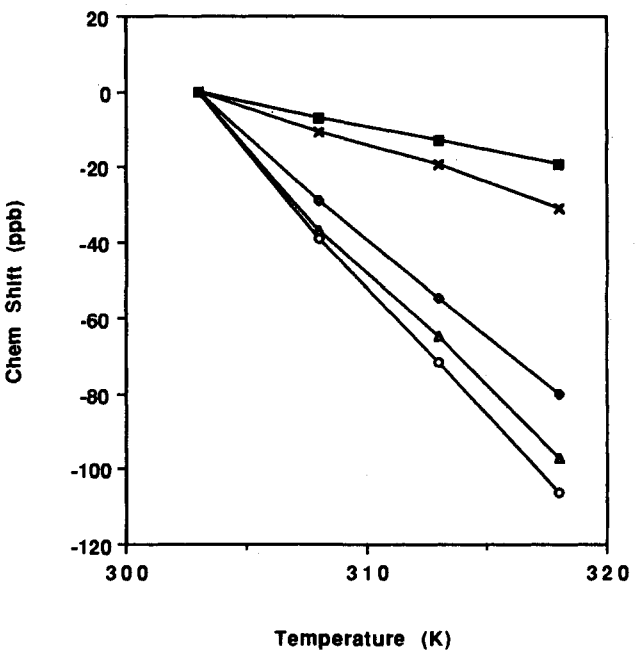

Figure 4. Chemical shifts of NH protons of BE18257B as function of temperature. The data for D-Glu$_1$ (×), Ala$_2$ (○), D-allo-Ile$_3$ (□), Leu (◇), and D-Trp$_5$ (△) are shown.

In addition to the NOE and coupling information, a variable-temperature study was carried out in order to determine the susceptibility to temperature of the chemical shifts of the NH protons. Results of this study are shown in Figure 4. It is seen that two of the NH protons display low temperature coefficients (less than three parts per million per 1000 K), normally characteristic of a hydrogen-bonded interaction. The other three NH protons have

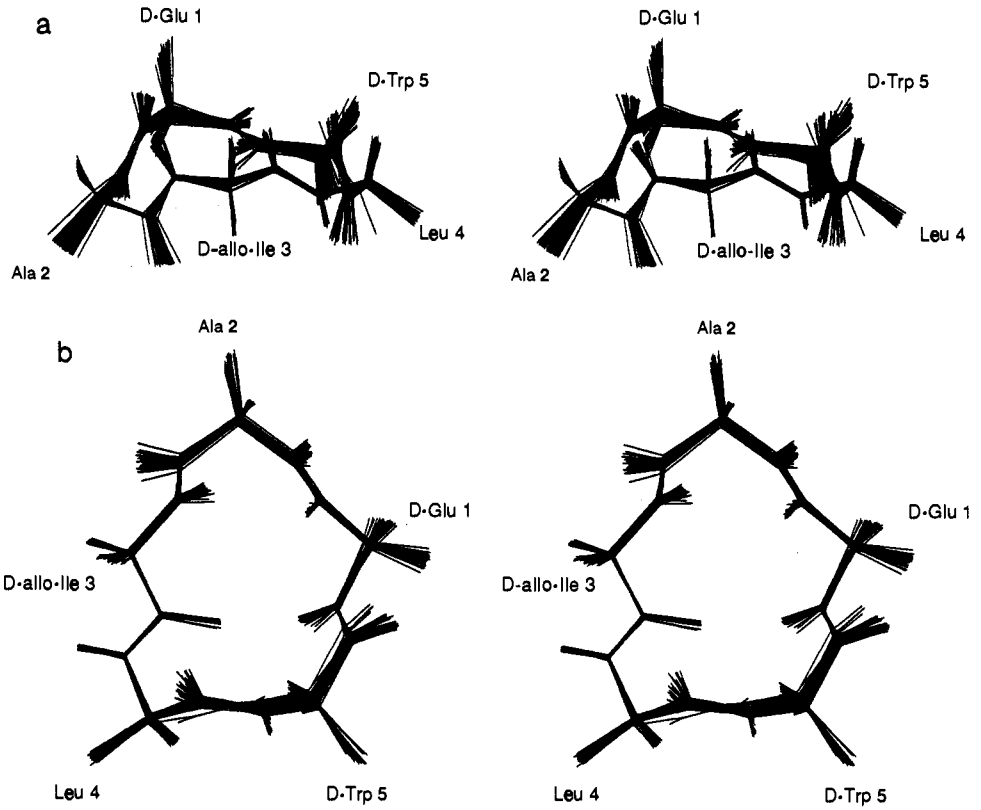

Figure 5. Stereoview of the 36 accepted structures resulting from the simulated annealing calculations, showing all heavy atoms. The backbone atoms have been superimposed resulting in a mean RMS of 0.12 ± 0.05 Å. Sidechain hydrogens have been omitted for clarity. Two views (a) from the side and (b) from above are shown.

magnitudes greater than three parts per million per 1000 K, suggesting that they are not involved in intramolecular hydrogen bonding interactions.

Structure Calculations. The simulated annealing calculations produced 40 structures, of which four were rejected on the basis of violating distance constraints, to produce a final set of 36 structures. These structures all converged to a similar backbone fold, thereby defining the likely conformation of the peptide. Stereoviews of this set superimposed on the basis of backbone atoms are shown in Figure 5a,b. The calculated conformation displays a bowl-shaped backbone with its longest axis on a line through Ala_2C_α and bisecting the Leu_4-Trp_5 peptide bond. The side chains of the three residues of D chirality project above the concave face of the bowl, with those residues of L chirality on the convex face. This arrangement of the backbone is such that the side chains of residues separated by two in the sequence are distant, except for Glu_1 and Ile_3, which are of like chirality and lie across the narrowest axis of the bowl. Initial calculations indicated the presence of two intramolecular hydrogen bonds corresponding to the two amide protons having small temperature coefficients. The H-bonds Glu_1HN to Ile_3O and Ile_3HN to Glu_1O form two recognizable elements of secondary structure, namely a type-II β-turn about Leu_4 and Trp_5 and an inverse γ-turn about Ala_2. These H-bonds were included in further simulations by constraining the acceptor to donor distances within the range 1.58–2.30 Å. Average H-bond lengths in the final set were 2.05 and 2.23 Å for the β- and γ-turns, respectively.

The calculated structures showed very good agreement with the experimental data, with no single structure having any violation of NOE constraints of more than 0.1 Å and the majority of structures having no violation of more than 0.05 Å. The level of convergence of the structures can be quantified by mean root mean square (rms) deviations calculated as the average of all possible pairwise comparisons, giving 0.12 ± 0.05 Å and 1.45 ± 0.25 Å for comparisons based on backbone and all heavy atoms, respectively.

Angular order parameters[24] provide an additional measure of the variation between structures of individual torsion angles. Values of the parameter range from 0 to 1, with a value of 1 indicating complete convergence of structures and a value of zero a random distribution. Table III lists the average torsion angles and angular order parameters for all backbone torsions and side chain χ_1 angles where appropriate. The peptide bonds which flank the inverse γ-turn, Ala_2 and Glu_1, are significantly nonplanar, presumably due to strain being introduced by the ring size. The angular order parameters for these two torsions and for $Ala_2\phi$ and ψ approach 1, indicating the high level of agreement between structures in this segment. The values for the angular order parameters for χ_1 of Ile_3, Leu_4, and Trp_5 show a good level of convergence for these side chains; in particular, the space occupied by the indole ring system of Trp_5 is well-defined. The χ_1 value for Trp_5 is in agreement with the previously mentioned analysis of $^3J_{H\alpha\text{-}H\beta}$ coupling constants, which suggested that the $\chi_1 = +60°$ rotamer was populated in excess of 80%. The χ_1 angle of Glu_1 is evenly distributed between the three staggered rotamers. Although some calculated structures indicate the formation of a hydrogen bond from the side chain carboxyl of this residue to the Trp_5H_N, experimental evidence, i.e., the chemical shift equivalence of both the H_β and H_γ proton pairs of Glu_1, indicates this is not a dominant conformation. Table III also includes the standard torsion angles for type-II β- and inverse γ-turns.[25] The $Ala_2\phi$ and ψ torsion angles closely match those for the

Table III. Average Torsion Angles[a] and Angular Order Parameters[b] (in Parentheses) for BE18257B and Ideal Torsion Angles for Standard Turns

	BE18275B				β-turn		γ-turn	
	ϕ	ψ	Ω	χ_1	ϕ	ψ	ϕ	ψ
Glu_1	148 (0.99)	−97 (0.99)	172 (1.00)	[c] (0.27)				
Ala_2	−74 (1.00)	82 (1.00)	−169 (1.00)				−80	70
Ile_3	91 (0.99)	−148 (1.00)	179 (1.00)	−53 (0.99)				
Leu_4	−61 (1.00)	103 (0.99)	177 (1.00)	−166 (0.97)	−60	120		
Trp_5	109 (0.98)	6 (0.99)	180 (1.00)	80 (0.94)	90	0		

[a] Torsion angle value taken from the "average" of the final 36 structures. [b] Well-converging structures have angular order parameters approaching 1. [c] An average value is not included for Glu_1 due to the wide distribution of values for this angle.

standared inverse γ-turn. Torsion angles in the type-II β-turn also agree within ±20° of the standard values.

Adequate sampling of conformational space is critical to structure determination by computational procedures incorporating distance constraints. In the case of a small, cyclic peptide where the range of conformational space may be expected to be small, it is also important to know how effective experimental constraints are in determining the structure. It could be anticipated that some elements of the calculated conformation are predetermined by the nature of the system, rather than conferred by the experimental constraints. Both these issues can be addressed by performing calculations where some or all experimental constraints are ignored, allowing the system to explore the full range of conformations available under the conditions of the simulation. To this end, two sets of 20 structures were obtained where first only NOE and then neither dihedral nor NOE constraints were included. These sets are referred to as NOE and FREE, respectively. Ramachandran plots of the resulting structure sets are shown in Figure 6, together with a plot of a set of 20 structures representative of the final 36, referred to as SA. Data from the FREE structure set show a wide spread of values of all torsion angles, indicating good sampling of conformational space. This wide range of conformations may be surprising, given the nature of the system. However, examination of the structures in this set shows that most of the variation in backbone torsion angles is due to the correlated rotation of the angles ϕ_i and ψ_{i-1}. This type of rotation results in large changes in local geometry through rotation of the plane formed by the peptide bond, while having little effect on the global geometry of the peptide backbone. Thus, a wide range of values is available to all torsion angles, even where the range of global geometries is restricted.

The NOE structure set in Figure 6 shows that NOE constraints alone are the major influence in determining the final structure. Under the influence of just these constraints, only two torsions remain undefined, i.e., $Ala_2\phi$ and D-$Glu_1\psi$. These are separated into two families, with convergence to a single structure limited only because both the intra- and interresidue Glu_1H_N–H_α NOESY cross-peaks are unquantifiable due to overlap. The addition of the dihedral constraints and formation of the inverse γ-turn hydrogen bond during the refinement processes is sufficient to tightly define the solution conformation around these torsion angles, as demonstrated by the data for the SA structures in Figure 6.

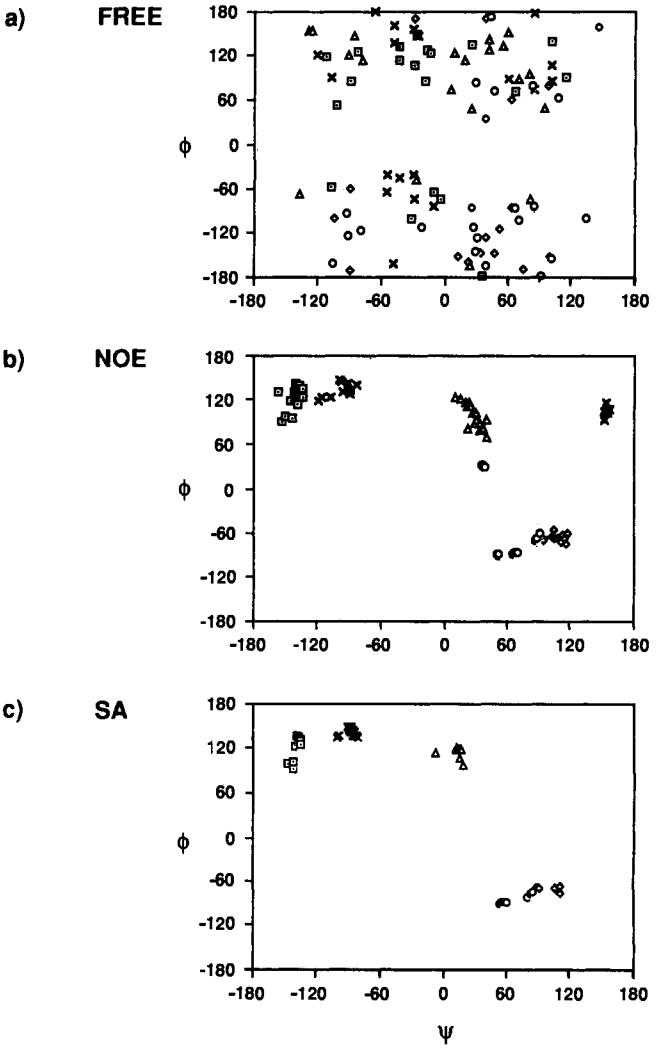

Figure 6. Ramachandran plots (ϕ vs ψ) for the three data sets. (a) FREE: no constraints were included in the simulated annealing calculation. (b) NOE: only the NOE-derived distance constraints were included. (c) SA: NOE-derived distance and dihedral constraints were both included in the calculations. The legend for all three data sets is (×) D-Glu_1, (○) Ala_2, (□) D-allo-Ile_3, (◇) Leu_4, (△) D-Trp_5.

IV. Discussion

The conformation calculated for the peptide backbone, comprising a type-II β-turn and an inverse γ-turn, is one that has been previously observed in cyclic pentapeptides. First observed in the crystal structure[18] of cyclo(Gly-Pro-Gly-D-Ala-Pro) and in solution,[26] this hydrogen bonding pattern has since been shown to be common for peptides which (like BE18257B) have alternating D and L chirality amino acids.[27] These data on related cyclic peptides provided support for the conformation of BE18257B proposed in the current study on the basis of experimental NMR data.

Very recently, a report on the structure of BE18257B based on *in vacuo* molecular modeling appeared in the literature.[28] Similarly, structures of BQ123 derived using various NMR approaches[29–31] appeared while the current report was in preparation. BQ123 has the sequence cyclo-

Table IV. Experimental Conditions and Derived Backbone Torsion Angles for BE18257B and BQ123

peptide	solvent	exptl condns: temp (K)	pH	T_c $1H_N/3H_N$[a] (ppb/°C)	$^3J_{\alpha\text{-}HN}$ (4/5)[b] (Hz)	ref
BQ123	20% CH_3CN	298	6.9	−4.5/−2.0	9.9/5.1	Atkinson and Pelton[29]
BQ123	20% CH_3CN	298	3.2	−3.7/−1.8		Atkinson and Pelton[29]
BQ123	DMSO	295		−2.0/−0.1	10.5/5.2	Atkinson and Pelton[29]
BQ123	60% glycol	310	3[c]	−3.40/−0.98	9.9/5.0	Krystek *et al.*[30]
BQ123	60% TFE	295	3[c]	−3.45/−1.76	9.9/5.0	Krystek *et al.*[30]
BQ123	DMSO	295		−1.90/−0.34	10.3/5.8	Krystek *et al.*[30]
BQ123	20% CH_3CN	298	5.4	[d]	9.6/5.2	Reily *et al.*[31]
BE18257B	DMSO	293		−2.0/−1.3	9.5/6.3	this study

	torsion angles (ϕ/ψ): Asp_1 or Glu_1	Pro_2 or Ala_2	Val_3 or Ile_3	Leu_4	Trp_5	structure[e]	
BQ123[f]	140/−90	−75/85	100/−100	−80/180	80/50	γ'/βII	Atkinson and Pelton[29]
BQ123[f]	150/−94	−81/51	128/−126	−76/107	81/27	γ'/βII	Krystek *et al.*[30]
BQ123[g]	145/−128	−78/82	123/−47	−166/100	84/29	γ	Reiley *et al.*[31]
BE18257B[f]	148/−97	−74/82	91/−148	−61/103	109/6	γ'/βII	this study
BE18257B[h]						γ	Satoh and Barlow[28]

[a] Temperature coefficients for the amide protons of residues 1 and 3 proposed to be involved in hydrogen bonds. [b] H_α–H_N coupling constants for residues 4 and 5 (proposed β-turn). [c] Approximate values only reported. [d] Reported as times for disappearance on D_2O exchange. $1H_N$ = 30 min, $3H_N$ = 180 min. [e] Reported turns, γ = γ turn (type not specified), γ' = inverse γ turn, βII = type-II β-turn. [f] Average torsion angles for structures calculated. [g] Torsion angles for lowest energy structure. [h] Torsion angles not reported; similar results were reported for BQ123.

(D-Trp-D-Asp-Pro-D-Val-Leu), closely homologous to BE18257B, and is the most potent cyclic pentapeptide ET_A antagonist reported to date.[32] Because of the importance of this class of peptides, and because there are some differences in conformations derived by different groups, it is of interest to compare the reported structures prior to relating them to homologous regions of the endothelins. Table IV summarizes the various experimental and theoretical studies and provides a comparison of key torsion angles for the peptide backbone.

The most extensive studies involve the combination of experimental NOE, coupling constant, and amide-exchange NMR data for BQ123 (Atkinson and Pelton[29] and Krystek et al.[30]) and BE18257B (reported herein). These studies are in agreement on the presence of a type-II β-turn and an inverse γ-turn in the peptide backbone. In the report by Satoh and Barlow[28] on both BE18257B and BQ123 using molecular modeling, the calculated backbone structures were very similar to one another, involving an inverse γ-turn about residue 2 (Ala or Pro). However, in contrast to the current study and those of Atkinson and Pelton[29] and Krystek et al.,[30] no β-turn was observed in either peptide. Satoh and Barlow[28] noted that their data were consistent with those presented by Reily et al.,[31] who did not report a β-turn. It is interesting to note that the structure derived by Reily et al. for BQ123 was based only on considerations of ^1H–^1H and ^1H-^{13}C coupling constants and not NOE data. While no β-turn was mentioned, their data did show a low-temperature coefficient for the amide proton of Asp_1, consistent with its involvement in hydrogen bonding, as would be expected for a β-turn. From these data it can be concluded that the likely conformation of these molecules does in fact include both a type-II β-turn and an inverse γ-turn. The failure of a purely theoretical approach[28] to predict a β-turn is not surprising, based on earlier findings which showed that β-turns are difficult to stabilize in theoretical simulations done in the absence of solvent.[27,33] The other conclusion to emerge is that the backbone conformations of BQ123 and BE18257B are remarkably similar to each other. Table IV illustrates that this similarity (as reflected in temperature coefficients, coupling constants, and derived torsion angles) occurs over a range of solvent conditions.

The similarity in structure of the peptides, and the availability of activity data which varies with the type of amino acid substitution,[32] means that the relationship of the solution conformations of the cyclic pentapeptides with their activities as potent, selective ET_A antagonists can be examined. This discussion is made with reference to the structure of the endothelins, which consists of two regions: a bicyclic core comprising residues 1–15 and a C-terminal tail.

There is considerable homology between BE18257B and the C-terminal pentapeptide of the endothelin family of peptides (ET-1, ET-2, ET-3, VIC, and the sarafotoxins), suggesting that BE18257B may mimic this region of the active peptides. This suggestion is reinforced by the observation that Trp_{21} of the endothelin family of peptides is necessary for binding at both ET_A and ET_B receptors. Additionally, it is possible that the aliphatic side chains of D-allo-Ile_3 and Leu_4 in BE19257B interact with the same functional groups of the ET_A receptor as Ile_{19} (or Val_{19}) and Ile_{20} in the endothelins. NMR studies on the solution structure of enothelins have suggested that the methyl groups of Ile_{19} are in close proximity to the indole moiety of the tryptophan, resulting in a dramatic upfield shift of the γ-methyl resonance.[5,6,34] In the current study, and in the three NMR studies of BQ123,[29-31] a similar upfield shift of one of the $Leu_4\delta$ methyl groups is observed. It may therefore be suggested that a hydrophobic methyl group in close proximity to the Trp moiety is a structural requirement for activity at the ET_A receptor.

In addition to the requirement for Trp_{21} and the hydrophobic methyl group, it has also been shown that the charge of the terminal carboxylate is important for binding of the endothelins.[35] Since BE18257B lacks a terminal charge, it has been postulated that the side chain carboxylate of D-Glu_1 could mimic this functionality.[32] The solution structure derived in this study does not indicate a preferred conformation for the D-Glu_1 side chain, but some indication of the importance of the position of this group may be seen by noting that the point substitution of D-Glu_1 with D-Asp_1, an amino acid with fewer degrees of conformational freedom, results in a 25-fold increase in activity.[32] Recent conformational studies on BQ123 have shown that a single side chain conformation for D-Asp_1 is

likely.[29-31] These results suggest that it is preferable for the charge to be either closer to the tryptophan side chain or more conformationally restricted for increased activity as an ET_A antagonist.

Substitution of proline for Ala_2 results in a 5-fold increase in activity as an ET_A receptor antagonist.[32] However, as has been discussed previously, the global fold of the backbones of BE18257B and BQ123 are very similar. The increase in activity cannot therefore be attributed to major conformational differences between the peptides and must instead be related to a decrease in conformational flexibility induced by the proline or to additional binding interactions of the proline.

One difficulty in correlating the activity of these cyclic pentapeptides as specific ET_A antagonists exclusively with the C-terminal region of the endothelins is that this region of the endothelin family of peptides is highly homologous (the C-terminal hexapeptide of ET-1, ET-2, ET-3, and VIC being identical), and yet the selectivity of the endothelins for the ET_A/ET_B receptors is quite different.[36] Such differential binding could be due to specific interactions of nonhomologous residues in the bicyclic core (residues 1–15) with the receptor. Alternatively, variations in these residues could result in differences in the conformation of the C-terminal tail or in its orientation with respect to the bicyclic core. Support for the latter possibility derives from NMR studies which show differences in the conformations of ET-1 and ET-3. ET-1 does not have a single, well-defined conformation of the C-terminal tail,[6,34] whereas in ET-3 the C-terminal hexapeptide is in close apposition to the extended helical region between Lys_9 and Cys_{15}.[37] Further evidence that the endothelin core may influence the tail conformation is that a rabbit antiserum raised against the terminal hexapeptide common to ET-1, ET-2, ET-3, and VIC showed different binding affinities to ET-1, ET-2, and ET-3.[38] It is therefore likely that the selectivity of the different endothelins to ET_A and ET_B receptors reflects subtle differences in the conformation of the C-terminus, resulting from differences in the bicyclic core. The specificity of the cyclic peptide antagonists would appear to derive from their ability to mimic a single conformation of the C-terminal region of endothelin-related peptides.

The proposal that the cyclic pentapeptide antagonists of ET_A derive their activity from their ability to mimic the C-terminal of the endothelins is preferred to the alternative hypothesis raised by Satoh and Barlow[28] that they mimic a loop comprising residues 6–8. Their hypothesis was based on a perceived similarity between residues 4, 5, and 1 (Leu, Trp, D-Asp or D-Glu) of the calculated cyclic pentapeptide structure and the structure of ET-1 determined in DMSO by Endo et al.[3] However, as noted previously, the structures for BE18257B and BA123 calculated by Satoh and Barlow do not display a β-turn. A recent study of the structure of ET-1[6] in aqueous ethylene glycol indicates that residues 5–8 are involved in a type-I β-turn. Superimposition of the type-II β-turn (residues 3, 4, 5, and 1) of BE18257B, as calculated in the current study, and the type-I β-turn in ET-1 show that a clearly different side chain spatiality exists in the two molecular fragments, especially for residues of unlike chirality.

Structure–activity studies on the cyclic pentapeptides also argue against the hypothesis that they mimic residues 6–8 of the endothelins. Satoh and Barlow[28] propose a recognition site for the 6–8 loop consisting of two hydrophobic sites which interact with residues 6 and 7 of the endothelins and a third site which interacts specifically with the carboxyl charge of Asp_8. There is considerable variation in the sequences of the endothelins at residues 6 and 7. ET-1 and ET-2, which are equipotent at the ET_A receptor, have Leu,Met and Trp,Leu in these positions, respectively. The first hydrophobic site must therefore bind to both Leu (ET-1 and the cyclic pentapeptides) and Trp (ET-2) and the second must bind Met (ET-1), Leu (ET-2), or Trp (cyclic pentapeptides). These hydrophobic sites would be nonspecific, interacting equally well with both aromatic and aliphatic side chains. This description of the binding of the cyclic pentapeptides to the ET_A receptors is not in keeping with the profile of activity observed for analogous peptides.[39] Substitutions of D-Phe or D-Leu for $D\text{-}Trp_5$ in BQ123 result in a loss of binding affinity by factors of 10 and greater than 100, respectively, whereas the substitution of Ala led to complete loss of activity. By contrast, the structure–activity data[39] for the cyclic pentapeptides are consistent with the hypothesis that they mimic the C-terminal region. In particular, the specific importance of the aromaticity of the Trp_5 residue in the cyclic pentapeptides correlates with the necessity of the aromaticity of Trp_{21} in the endothelins. Point replacement of Trp_{21} in ET-1 with Tyr or Phe yields losses in activity by factors of approximately 2.5 and 5, respectively.[40] An analogue where Trp_{21} was replaced by Ala was completely inactive.

In conclusion, the NMR and simulated-annealing studies have shown that the backbone of BE18257B exists with a well-defined type-II β-turn (around positions 4 and 5) and one inverse γ-turn which has alanine at its apex. It is likely that the antagonistic activity of BE18257B may be correlated to regions of the receptor that interact with the C-termini of the endothelin peptides.

Acknowledgment. This work was supported in part by a grant from the Australian Research Council. We acknowledge the support of Auspep Pty Ltd. and thank the Victorian Education Foundation for a scholarship for V.S. We also thank Jacqui King for her excellent work in preparing the manuscript.

Supplementary Material Available: Atomic coordinates in pdb format for a conformation for BE19257B calculated in this study (2 pages). Ordering information is given on any current masthead page.

References

(1) Doherty, A. Endothelin: A New Challenge. *J. Med. Chem.* **1992**, *9*, 1493–1508.
(2) Saudek, V.; Hoflack, J.; Pelton, J. T. ^1H NMR Study of Endothelin, Specific Sequence Assignment of the Spectrum and a Solution Structure. *FEBS Lett.* **1989**, *257*, 145–148.
(3) Endo, S.; Inooka, H.; Ishibashi, Y.; Kitada, C.; Mizuta, E.; Fujino, M. Solution Conformation of Endothelin determined by Nuclear Magnetic Resonance and Distance Geometry. *FEBS Lett.* **1989**, *257*, 149–154.
(4) Munro, S. L.; Craik, D. J.; McConville, D.; Hall, J. G.; Searle, M.; Bicknell, W.; Scanlon, D.; Chandler, C. Solution Conformation of Endothelin, a Potent Vasoconstricting Bicyclic Peptide. A Combined Use of ^1H NMR Spectroscopy and Distance Geometry Calculations. *FEBS Lett.* **1991**, *278*, 9–13.
(5) Tamaoki, H.; Kobayashi, Y.; Nishimura, S.; Ohkubo, T.; Kyoguku, Y.; Nakajima, K.; Kumagaye, S.; Kimura, T.; Sakakibara, S. Solution Conformation of Endothelin determined by means of ^1H NMR Spectroscopy and Distance Geometry Calculations. *Prot. Eng.* **1991**, *4*, 509–518.
(6) Andersen, N. H.; Chen, C.; Marschner, T. M.; Krystek, S. R., Jr.; Bassolino, D. Conformational Isomerism of Endothelin in Acetic Acid Media: A Quantitative NOESY Analysis. *Biochemistry* **1992**, *31*, 1280–1295.

(7) Nakajima, S.; Niiyama, K.; Ihara, M.; Kojiri, K.; Suda, H. Endothelin-Binding Inhibitors, BE18257A and BE18257B: II. Structure Determination. *J. Antibiot.* 1991, *44*, 1348–1356.
(8) Miyata, S.; Fukami, N.; Neya, M.; Tokase, S.; Kiyoto, S. WS-7338, New Endothelin Receptor Antagonist Isolated from *Streptomyces* sp. No. 7338: Structure of WS-7388 A, B, C and D and Total Synthesis of WS-7288B. *J. Antibiot.* 1992, *45*, 788–791.
(9) Ihara, M.; Fukuroda, T.; Saeki, T.; Nishikibe, M.; Kojiri, K.; Suda, H.; Yano, M. An Endothelin Receptor (ET_A) Antagonist isolated from *Streptomyces misakiensis*. *Biochem. Biophys. Res. Commun.* 1991, *178*, 32–137.
(10) Ihara, M.; Noguchi, K.; Saeki, T.; Fukuroda, T.; Tsuchida, S.; Kimura, S.; Fukami, T.; Ishikawa, K.; Nishikibe, M.; Yano, M. Biological Profiles of Highly Potent novel Endothelin Antagonists selective for the ET_A Receptor. *Life Sci.* 1991, *50*, 247–255.
(11) Atherton, E.; Logan, C. L.; Sheppard, R. C. Peptide Synthesis Procedure for Solid-Phase Synthesis using N^{α}-Fluorenyl Methocarbonyl Amino Acids on Polyamide Supports. *J. Chem. Soc., Perkin Trans. 1* 1981, 538.
(12) Wang, S. S. *p*-Alkoxybenzyl Alcohol Resin and Alkoxybenzyloxycarbonyl Hydrazide Resin for Solid-Phase Synthesis of Protected Peptide Fragments. *J. Am. Chem. Soc.* 1973, *95*, 1328–1331.
(13) Rance, M.; Sørensen, O. W.; Bodenhausen, G.; Wagner, G.; Ernst, R. R.; Wüthrich, K. Two-Dimensional Double Quantum ^1H NMR Spectroscopy of Proteins. *Biochem. Biophys. Res. Commun.* 1983, *117*, 479–485.
(14) Macura, S.; Ernst, R. R. Eucidation of Cross-Relaxation in Liquids by Two-Dimensional NMR Spectroscopy. *Mol. Phys.* 1980, *41*, 91–117.
(15) Braunschweiler, L.; Ernst, R. R. Coherence Transfer by Isotropic Mixing; Application to Proton Correlation Spectroscopy. *J. Magn. Reson.* 1983, *53*, 521–528.
(16) Hare Research, Inc., 18943 120th Avenue N.E., Suite 104, Bothell, WA 98011.
(17) Brünger, A. T. *XPLOR Manual*; Yale University: New Haven, CT, 1990.
(18) Karle, I. L. Crystal Structure and Conformation of Cyclo-(Glycylprolylglycl-D-Alanylprolyl) containing 4→1 and 3→1 Intramolecular Hydrogen Bonds. *J. Am. Chem. Soc.* 1978, *100*, 1286–1289.
(19) Mierke, D. M. F.; Kessler, H. Molecular Dynamics with Dimethyl Sulphoxide as Solvent. Conformation of a Cyclic Hexapeptide. *J. Am. Chem. Soc.* 1991, *113*, 9466–9470.
(20) Wüthrich, K. *NMR of Proteins and Nucleic Acids*; John Wiley: New York, 1986.
(21) Brown, L. R.; Farmer, B. T. The rotating frame Overhauser effect. *Methods Enzymol.* 1980, *176*, 199–216.
(22) Wagner, G.; Braun, W.; Havel, T. F.; Schaumann, T.; Go, N.; Wüthrich, K. Protein Conformation by NMR and Distance Geometry. *J. Mol. Biol.* 1987, *196*, 611–639.
(23) Pachler, K. G. R. Nuclear Magnetic Resonance Study of Some α-Amino Acids–II. Rotational Isomerism. *Spectro. Chimica Acta* 1964, *20*, 581–587.
(24) Detlefsen, D. J.; Thanabal, V.; Pecoraro, V. L.; Wagner, G. Solution Structure of Fe(II) Cytochrome c551 from *Pseudomonas aeruginosa* as determined by Two-Dimensional ^1H NMR. *Biochemistry* 1991, *30*, 9040–9046.
(25) Rose, G. D.; Gierasch, L. M.; Smith, J. A. Turns in Peptides and Proteins. *Adv. Peptide Protein Chem.* 1985, *37*, 1–107.
(26) Pease, L. G.; Watson, C. Conformational and Ion Binding Studies of a Cyclic Pentapeptide. Evidence for β- and γ-Turns in Solution. *J. Am. Chem. Soc.* 1978, *100*, 1279–1286.
(27) Stradley, S. J.; Rizo, J. R.; Bruch, M. D.; Stroup, A. N.; Gierasch, L. M. Cyclic Pentapeptides as Models for Reverse Turns: Determination of the Equilibrium Distribution between Type I and Type II Conformations of Pro-Asn and Pro-Ala β-Turns. *Biopolymers* 1990, *29*, 263–287.
(28) Satoh, T.; Barlow, D. Molecular Modelling of the Structures of Endothelin Antagonists. Identification of a Possible Structural Determinant for ET_A Receptor Binding. *FEBS Lett.* 1992, *310*, 83–87.
(29) Atkinson, R. A.; Pelton, J. T. Conformational study of cyclo[D-Trp-Asp-Pro-D-Val-Leu] and the endothelin-A receptor-selective antagonist. *FEBS Lett.* 1992, *296*, 1–6.
(30) Krystek, S. R., Jr.; Bassolino, D. A.; Bruccoleri, R. E.; Hunt, J. T.; Porubcan, M. A.; Wandler, C. F.; Andersen, N. H. Solution conformation of a cyclic pentapeptide endothelin antagonist. Comparison of structures obtained from constrained dynamics and conformational search. *FEBS Lett.* 1992, *299*, 255–261.
(31) Reily, M. D.; Thanabal, V.; Omecinsky, D. O.; Dunbar, J. B.; Doherty, A. M.; DePue, P. L. The solution structure of a cyclic endothelin antagonist, BQ-123, based on ^1H–^1H and ^{13}C–^1H three-bond coupling constants. *FEBS Lett.* 1992, *300*, 136–140.
(32) Ishikawa, K.; Fukami, T.; Nagase, T.; Fujita, K.; Hayama, T.; Niiyama, K.; Mase, T.; Ihara, M.; Yano, M. Cyclic Pentapeptide Endothelin Antagonists with High ET_A Selectivity. Potency and Solubility Enhancing Modifications. *J. Med. Chem.* 1992, *35*, 2139–2142.
(33) Kitson, O. H.; Hagler, A. T. Theoretical Studies of the Structure and Molecular Dynamics of a Peptide Crystal. *Biochemistry* 1988, *27*, 5246–5257.
(34) Krystek, S. R.; Bassolino, D. A.; Novotny, J.; Chen, C.; Marschner, T. M.; Andersen, N. H. Conformation of Endothelin in Aqueous Ethylene Glycol determined by ^1H NMR and Molecular Dynamics Simulations. *FEBS Lett.* 1991, *281*, 212–218.
(35) Kimura, S.; Kasuya, Y.; Sawamura, T.; Shinmi, O.; Sugita, Y.; Yanagisawa, M.; Gato, K.; Masaki, T. Structure–Activity Relationships of Endothelin: Importance of the C-Terminal Moiety. *Biochem. Biophys. Res. Commun.* 1988, *156*, 1182–1186.
(36) Saeki, T.; Ihara, M.; Fukuroda, T.; Yamagiwa, M.; Yano, M. [$Ala^{1,3,11,15}$] Endothelin-1 Analogs with ET_B Agonist Activity. *Biochem. Biophys. Res. Commun.* 1991, *179*, 286–292.
(37) Mills, R. G.; O'Donoghue, S. I.; Smith, R.; King, G. F. Solution Structure of Endothelin-3 determined using NMR Spectroscopy. *Biochemistry* 1992, *31*, 5640–5645.
(38) Löffler, B-M.; Jacot-Guillarmod, H. A Rabbit Antiserum raised against the Hexapeptide Endothelin (16–21) shows Different Binding Affinities for Endothelin-1, -2, and -3. *Life Sci.* 1992, *50*, 2001–2009.
(39) Maeji, N. J.; Valerio, R. M.; Bray, A. M.; Geysen, H. M.; Spellmeyer, D. C.; Stauber, G. B.; Kaufman, S. E.; Brown, S. A.; Moos, W. H. Simultaneous Multiple Peptide Synthesis: Screening for Endothelin Receptor Ligands. Proceedings of the Royal Australian Chemical Institute, 9th National Convention, Dec 1992.
(40) Watanabe, T. X.; Itahara, Y.; Nakajima, K.; Kumagaye, S.; Kimura, T.; Sakakibara, S. The Biological Activity of Endothelin-1 Analogues in Three Different Assay Systems. *J. Cardiovasc. Pharmacol.* 1991, *17*, S5–S9.